Heterogeneity and Pliability of Tumor-educated Macrophages

Ryan D. Roberts*

Many characteristics that define malignant tumors (Hanahan, and Weinberg, 2000) arise from their ability to change the way that cells around them respond. They learn to generate signals that cause otherwise normal cells to behave in ways that suit their proliferative and metastatic tendencies. They convince blood vessels to grow, they turn off killer immune cells, and they elicit growth signals from cells that otherwise wouldn't provide them.

One type of immune cell that often succumbs to tumor manipulation is the macrophage. Since Virchow in 1863, scientists have recognized that these inflammatory cells did something to tumors that made things worse for patients. Modern clinical science has uncovered strong links between these inflammatory cells and patient outcomes (Kacinski, 1995; Scholl, Lidereau, et al, 1996). Basic scientists have shown how breast tumors revert to developmental programs that invoke reciprocal macrophage-tumor interactions which enable tumor cell growth and survival as well as spread of these cells to other parts of the body (Condeelis, and Pollard, 2006).

Other scientists have noted that macrophages and other classical cell types actually demonstrate a number of diverse phenotypes. Tacke and colleagues (Tacke, and Randolph, 2006) have identified different subpopulations of monocytes (which are blood-borne macrophage precursors), each of which behave differently and respond differently to various challenges. These monocyte subsets have been characterized primarily using the Gr-1 antigen, with the

* Room 201 DHLRI, 473 W. 12th Ave, Columbus, OH 43212. I would like to thank Clay Marsh for his guidance while completing this project. I also thank Randall Evans, Tim Eubank, Julie Roda and Jennifer Curry for their help and advice. Thanks to Nick Sullivan and Brett Hall for their help with the tumor growth assays.

"classical," inflammatory monocytes identified by high Gr-1 surface expression. Recently, David Hume's group (Sasmono, Ehrnsperger, et al, 2007) showed that a particular subset of neutrophils transcribed genes typically associated with macrophages. This subset identified by their high Gr-1 expression. Other groups, working to characterize some of the bad macrophage players in tumor pathogenesis, have identified a subset of tumor associated macrophages which they have termed myeloid-derived suppressor cells (MDSCs) (Sica, and Bronte, 2007). Once again, this subset was delineated by high Gr-1 expression. There exists a possibility that these three cellular subsets may be intimately related.

In the present studies, we wanted to explore the effects of macrophage ablation in a tumor model and the effects of altering levels of particular cellular subsets on tumor growth and metastasis. To do this, we made use of a previously characterized mouse model, the MAFIA (macrophage fas-induced apoptosis) mouse (Burnett, Kershen, et al, 2004) (*Figure 1*). To create this mouse, Burnett and colleagues generated a construct which expressed an inducible suicide gene (Yang, Rozamus, et al, 2000) under the regulation of the M-CSF receptor promoter. Administration of an engineered ligand (AP20187 (Jin, Zeng, et al, 2000)) induces apoptosis of cells which express the suicide gene—in this case, the macrophage. This model provides us with a unique method for temporal ablation of mouse macrophages.

Results

Dimerizer administration effectively ablates tumor macrophages. We wanted to verify that activation of the suicide gene could eliminate macrophages from the tumors of MMTV-PyMT transgenic mice. To do so, we stained FFPE sections of tumors extracted from MAFIA-PyMT mice with antibodies directed at the F4/80 antigen. *Figure 2* shows the results of these

experiments. Both qualitative and quantitative analysis of these sections demonstrate a near-complete elimination of F4/80+ cells from the tumors. We note that macrophage numbers from the treated tumors always measure artificially high, since the macrophages that would normally destroy the F4/80+ apoptotic bodies have been eliminated. These data confirm the validity of this model as a method for testing the effects of macrophage ablation on tumor progression.

Macrophage ablation in MAFIA mice promotes tumor growth and metastasis. To test the effects of macrophage ablation, we randomized ten-week old PyMT+ mice with or without the MAFIA transgene to treatment with dimerizer (AP20187) or vehicle (dimerizer diluent, see Materials and Methods). After five weeks of treatment, we removed their tumors and weighed them to compare total tumor burden between groups. As a group, MAFIA+ mice that received dimerizer (macrophages ablated) had larger tumors that mice that did not have the MAFIA transgene or that did not receive dimerizer (macrophages normal, *Figure 3A*).

We removed the lungs from these same mice and mounted them whole, according to procedures outlined in Materials and Methods. We imaged these lungs under a stereomicroscope equipped with a lighted stage to count the metastases. Mice whose macrophages were ablated had significantly more metastases than mice with normal macrophage levels (*Figure 3B*).

Macrophage apoptosis does not stimulate tumor growth. One hypothesis proposed to explain the outcomes we observed is that massive apoptosis induced by administration of the dimerizer might create pools of apoptotic bodies that might stimulate tumor cells to grow and take on malignant characteristics. To test this hypothesis, we performed three-dimensional tumor growth assays (TGAs) (Sasser, Mundy, et al, 2007) with the aid of Dr. Brett Hall's lab at Nationwide Children's Hospital. *Figure 4A* shows data validating the use of the MET-1 cell line developed

in the Hall lab. *Figure 4B* shows the results of our experimental data. Tumor cells were cultured for the first 48 hours alone or together with increasing numbers of bone-marrow –derived macrophages from MAFIA+ mice. After 48 hours, we administered a dose of dimerizer to induce apoptosis in the macrophages. From the graph, one can see that this apoptosis (or the drug itself) actually caused a *decrease* in the rate of tumor cell growth. One can also see that, before treatment, tumor growth in this system decreased with increasing macrophage number.

This observation may stem from a crowding effect of the macrophages on the tumor cells, although this would be very unlikely, especially at the lower macrophage denisities. Taken in context with the other results shown in this study, these results suggest that some of the more mature macrophages may actually take on roles that negatively affect tumor growth.

Macrophage ablation causes reactive monocytosis and stimulates extramedullary hematopoiesis. We removed blood and spleens from the mice in an effort to further characterize the effects of macrophage ablation on the hematopoietic system in these mice. Spleens stained for F4/80 (*Figure 5A*) showed a reduction in the number of macrophages and disruption of the splenic architecture, as was previously described (Burnett, Kershen, et al, 2004). We also noted in these spleen samples several areas of extramedullary hematopoiesis (see arrows), suggesting a stimulus for blood cell production that could not be met by the bone marrow.

CBC analysis on blood samples from these mice (*Figure 5B*) showed that nucleated cells, band neutrophils, segmented neutrophils, lymphocytes, and platelets were not significantly different between MAFIA+ mice treated with dimerizer and those treated with vehicle. However, significantly lower hemoglobin and red cell counts showed that macrophage-depleted mice experienced relative anemia when compared to their vehicle-treated counterparts. Most

interestingly, dimerizer-treated mice demonstrated a marked reactive monocytosis, with a nearly 5-fold increase in blood monocyte levels.

Monocytic cells infiltrate tumors near blood vessels. While preliminary analysis of the F4/80-stained tumors showed a paucity of macrophages in the tumors of mice treated with AP20187, closer inspection told a more interesting story. Near areas of high blood vessel density (*Figure 6*), one could find relatively high numbers of F4/80+ cells migrating through the tumor. Most of these cells demonstrated a younger, more monocyte-like morphology (black-center arrows), and many of the cells which displayed more mature morphologic character showed signs of blebbing and apoptosis (white-center arrows).

Dimerizer treatment causes shift toward the classical, inflammatory, Gr-1^{hi} monocyte subtype. We have taken note of recent work describing the characteristics of monocyte subpopulations (Strauss-Ayali, Conrad, and Mosser, 2007; Tacke, and Randolph, 2006), and feel it may relate to studies in the realm of tumor biology. This work has shown that the Gr-1^{hi} monocytes exhibit many pro-inflammatory properties. If inflammation can drive cancer (Lin, and Karin, 2007), then any selection for or against this particular monocyte subset might affect tumor progression. Likewise, changes in the Gr-1hi, F4/80+ population within the tumor could also change the outcome (Sica, and Bronte, 2007). We therefore wanted to show how treatment with dimerizer affected these monocyte and tumor macrophage subpopulations. To do so, we isolated white blood cells from whole blood and from tumors collected from MAFIA+ mice treated with or without dimerizer. We then stained these cells with markers that delineated the different subpopulations. The results (*Figure 7*) show that treatment with dimerizer causes a shift toward the Gr-1^{hi} phenotype monocyte in the blood, and the Gr-1^{hi} MDSC in the tumor.

Discussion

Decades of studies have established that tumor-associated macrophages (TAMs) promote tumor progression by providing tumor growth factors (Lin, and Karin, 2007), blunting anti-tumor immune responses (Sica, and Bronte, 2007), and facilitating metastasis (Condeelis, and Pollard, 2006). Contrary to what we expected, our data show that elimination of macrophages by Fas-induced apoptosis actually accelerated tumor growth and increased metastasis.

We provide some evidence here that the mechanism underlying this observation may involve a reactive increase in a particular subset of cells. So, while we have reduced or eliminated the majority of macrophages within the tumor environment, we may have actually increased the numbers of one particular subset of cells.

While further study will be required to prove such a hypothesis, we suspect that these mesenchymal-derived stem cells, these Gr-1+ tumor associated macrophages, and the Gr-1hi inflammatory monocyte subset may be interrelated. If such were truly the case, this could provide interesting therapeutic opportunities. Our data suggest that it might be possible to eliminate the tumor-promoting activities of macrophages by targeting one particular subset. This would likely reduce potential side effects and could make such treatments more effective, if the anti-tumor behaviors of other macrophage subsets were preserved.

Materials and methods

Mice. MMTV-PyMT (Lin, Jones, et al, 2003) and MAFIA (Burnett, Kershen, et al, 2004) mice were obtained from Jackson Laboratories and bred at the animal facility at the Ohio State University College of Medicine. All experiments were conducted in accordance with protocols approved by the OSU Institutional Animal Care and Use Committee. Heterozygous PyMT+

male mice (on an FVB background) were bred to heterozygous or homozygous MAFIA+ female mice (on a B6 background). Only F1 animals from these crosses were used to ensure background consistency and genetic identity. Ear punch pieces were digested in accordance with the "Non-organic Tail DNA Extraction Protocol" published by Jackson Labs. Mice were identified by PCR of these samples using the following primers: PyMT-Fv3, 5'-AATCCTTGTGTTGCTGAGCCCGATG -3' and PyMT-Rv3, 5'-TCGAAATGAGCCCTCTGCAAATCCC -3', to amplify a 255bp product corresponding to a portion of the polyomavirus middle T antigen protein, or MAFIA-F, 5'- AAG TTC ATC TGC ACC ACC G -3' and MAFIA-R, 5'- TCC TTG AAG AAG ATG GTG CG -3' to amplify a 173bp product corresponding to the GFP portion of the transgene.

Dimerizer. AP20187 was kindly provided in lyophilized form by ARIAD Pharmaceuticals. This was reconstituted with 100% ethanol to give a final concentration of 50 mg/ml. This stock solution was separated into 50 μl aliquots and stored at -20°C. "Dimerizer diluent" was prepared by creating a solution containing 4% ethanol, 10% PEG-400, and 1.7% Tween-20 in milliQ water, then sterilizing by filtration. When ready for use, 50 μl aliquots were reconstituted with 950 μl of dimerizer diluent to make a 2.5 mg/ml "1X" solution for induction treatments. This concentration corresponds to a 100 ul dose for the average 25 gram mouse to receive 10 mg/kg. Maintenance doses were prepared by diluting this 1X solution 10-fold with dimerizer diluent.

Macrophage ablation. At 10 weeks ± 2 days of age, we randomized female PyMT+ mice with or without the MAFIA transgene to either dimerizer (AP20187, Ariad Pharmaceuticals) or vehicle treatment (dimerizer diluents) groups. This time corresponded with the first appearance of palpable tumors, as determined in preliminary studies. Treatment with dimerizer or vehicle

began at this time continued for five weeks. In accordance with the recommendations of the manufacturer, mice were treated with a five-day induction regimen consisting of daily tail vein injections at 10 mg/kg. After induction therapy, mice were treated with 1 mg/kg of AP20187 three times per week. The last dose of dimerizer was given the evening before sacrifice (12-16 hours prior).

Immunohistochemistry. After five weeks of treatment (at 15 weeks ±2 days of age), mice were euthanized and their organs harvested for analysis. Tumors and spleens were fixed in 10% NBF, then embedded in paraffin and sectioned. Optimal conditions for rat anti-mouse F4/80 (clone CI:A3-1, AbD Serotec) were protease digestion (protease 1, Ventana Medical Systems, Tucson AZ) for 4 minutes, dilutions of 1:100, dilution of the biotinylated anti-rat secondary antibody at 1:200, and use of the DAB detection system from Enzo Diagnostics (Farmingdale, NY). Total cell influx was analyzed by digital images captured of the entire tumors and quantified using Adobe Photoshop CS2 software.

Lung Whole Mounts. The methods we used for quantification of lung metastasis have been described previously (Jessen, Liu, et al, 2004). Briefly, lungs removed immediately after euthanization were insufflated with PBS to equivalent pressures, then fixed in 10% formalin. The lungs were whole mounted and stained with hematoxylin. These were then viewed under a steromicroscope to count the metastases, which appear as opacities in the cleared lung fields.

Tumor Growth Assays (TGAs). MET-1 Tumor cells (Borowsky, Namba, et al, 2005), a highly metastatic cell line derived from MMTV-PyMT mice, were stably transfected with a plasmid coding for DsRed. The remaining details of the TGAs have beed described in detail previously (Sasser, Mundy, et al, 2007).

Flow Cytometry. Blood samples were cleared of red blood cells by 5 minute incubations using RBC lysis buffer (eBioscience). Samples were pelleted then resuspended in FACS buffer containing FC Block (BD Pharmingen). These samples were stained with PE-Cy7 anti-mouse F4/80, PerCP-Cy5.5 anti-mouse Gr-1 (both from BioLegend) and PI (BD Pharmingen). Samples were then washed twice with FACS buffer and fixed with 1% paraformaldehyde. Samples were run on a BD FACSAria machine and analysis performed using FCS Express software.

For flow performed on tumor samples, pieces of tumor were minced in RPMI, then filtered through a cell strainer. Buffy layers containing mostly lymphocytes and monocytes were separated by centrifugation over a lymphocyte separation medium gradient (cellgro). These samples were then processed as described for blood.

Works Cited

Borowsky, A.D., Namba, R., Young, L.J., Hunter, K.W., Hodgson, J.G., Tepper, C.G., McGoldrick, E.T., Muller, W.J., Cardiff, R.D., and Gregg, J.P. (2005). Syngeneic mouse mammary carcinoma cell lines: two closely related cell lines with divergent metastatic behavior. Clin. Exp. Metastasis *22*, 47-59.

Burnett, S.H., Kershen, E.J., Zhang, J., Zeng, L., Straley, S.C., Kaplan, A.M., and Cohen, D.A. (2004). Conditional macrophage ablation in transgenic mice expressing a Fas-based suicide gene. J. Leukoc. Biol. *75*, 612-623.

Condeelis, J., and Pollard, J.W. (2006). Macrophages: obligate partners for tumor cell migration, invasion, and metastasis. Cell *124*, 263-266.

Hanahan, D., and Weinberg, R.A. (2000). The hallmarks of cancer. Cell (Cambridge) *100*, 57.

Jessen, K.A., Liu, S.Y., Tepper, C.G., Karrim, J., McGoldrick, E.T., Rosner, A., Munn, R.J., Young, L.J., Borowsky, A.D., Cardiff, R.D., and Gregg, J.P. (2004). Molecular analysis of metastasis in a polyomavirus middle T mouse model: the role of osteopontin. Breast Cancer Res. *6*, R157-69.

Jin, L., Zeng, H., Chien, S., Otto, K.G., Richard, R.E., Emery, D.W., and Blau, C.A. (2000). In vivo selection using a cell-growth switch. Nat. Genet. *26*, 64-66.

Kacinski, B.M. (1995). CSF-1 and its receptor in ovarian, endometrial and breast cancer. Ann. Med. *27,* 79-85.

Lin, E.Y., Jones, J.G., Li, P., Zhu, L., Whitney, K.D., Muller, W.J., and Pollard, J.W. (2003). Progression to malignancy in the polyoma middle T oncoprotein mouse breast cancer model provides a reliable model for human diseases 1. Am. J. Pathol. *163,* 2113-2126.

Lin, W.W., and Karin, M. (2007). A cytokine-mediated link between innate immunity, inflammation, and cancer. J. Clin. Invest. *117,* 1175-1183.

Sasmono, R.T., Ehrnsperger, A., Cronau, S.L., Ravasi, T., Kandane, R., Hickey, M.J., Cook, A.D., Himes, S.R., Hamilton, J.A., and Hume, D.A. (2007). Mouse neutrophilic granulocytes express mRNA encoding the macrophage colony-stimulating factor receptor (CSF-1R) as well as many other macrophage-specific transcripts and can transdifferentiate into macrophages in vitro in response to CSF-1. J. Leukoc. Biol. *82,* 111-123.

Sasser, A.K., Mundy, B.L., Smith, K.M., Studebaker, A.W., Axel, A.E., Haidet, A.M., Fernandez, S.A., and Hall, B.M. (2007). Human bone marrow stromal cells enhance breast cancer cell growth rates in a cell line-dependent manner when evaluated in 3D tumor environments. Cancer Lett. *254,* 255-264.

Scholl, S.M., Lidereau, R., de la, R.A., Le Nir, C.C., Mosseri, V., Nogues, C., Pouillart, P., and Stanley, F.R. (1996). Circulating levels of the macrophage colony stimulating factor CSF-1 in primary and metastatic breast cancer patients. A pilot study. Breast Cancer Res. Treat. *39,* 275-283.

Sica, A., and Bronte, V. (2007). Altered macrophage differentiation and immune dysfunction in tumor development. J. Clin. Invest. *117,* 1155-1166.

Strauss-Ayali, D., Conrad, S.M., and Mosser, D.M. (2007). Monocyte subpopulations and their differentiation patterns during infection. J. Leukoc. Biol. *82,* 244-252.

Tacke, F., and Randolph, G.J. (2006). Migratory fate and differentiation of blood monocyte subsets. Immunobiology *211,* 609-618.

Yang, W., Rozamus, L.W., Narula, S., Rollins, C.T., Yuan, R., Andrade, L.J., Ram, M.K., Phillips, T.B., van Schravendijk, M.R., Dalgarno, D., Clackson, T., and Holt, D.A. (2000). Investigating protein-ligand interactions with a mutant FKBP possessing a designed specificity pocket. J. Med. Chem. *43,* 1135-1142.

Figure 1

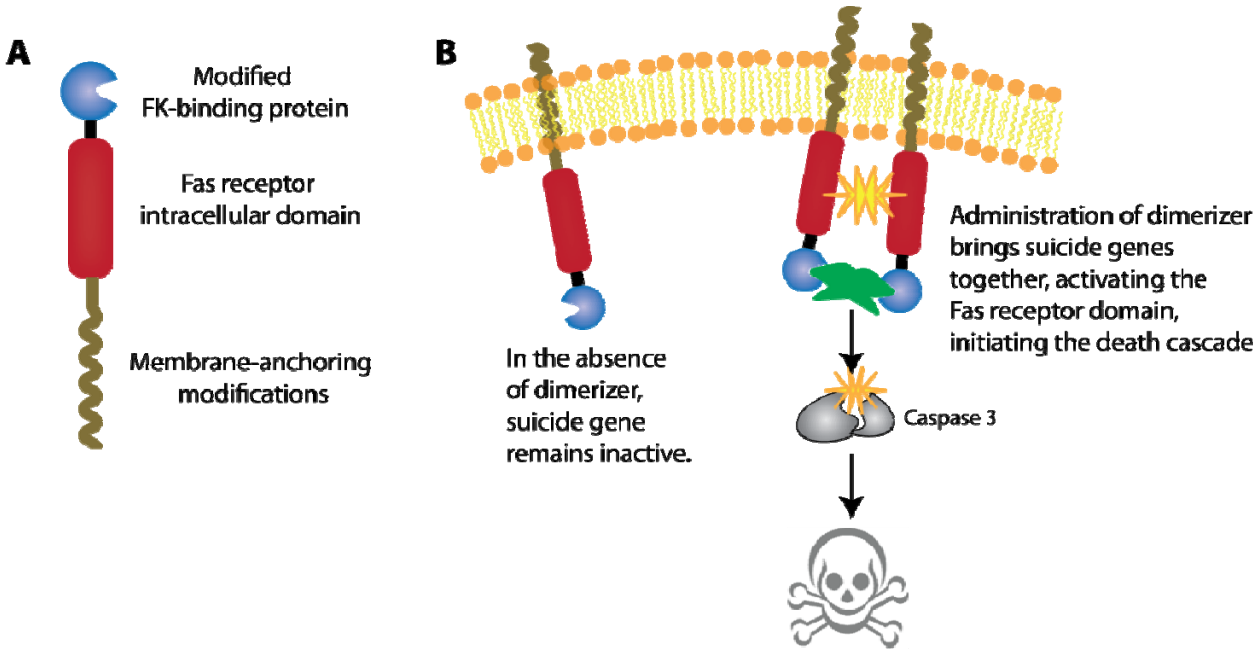

MAFIA mice. A) The suicide gene contains a modified FK-binding protein coupled with the signaling portion of the Fas receptor. The whole construct is anchored to the cell membrane by other modifications. In the MAFIA mice, expression of this gene is limited to macrophages and a subset of neutrophils by placing the gene under the control of the M-CSF receptor promoter (*fms*). B) In the absence of any dimerizing agent, the suicide gene remains inactive. Upon administration of the pharmaceutical dimerizing agent AP20187, crosslinking of the receptors occurs, activating the Fas receptor domain and initiating the death cascade through the activation of caspase 3.

Figure 2

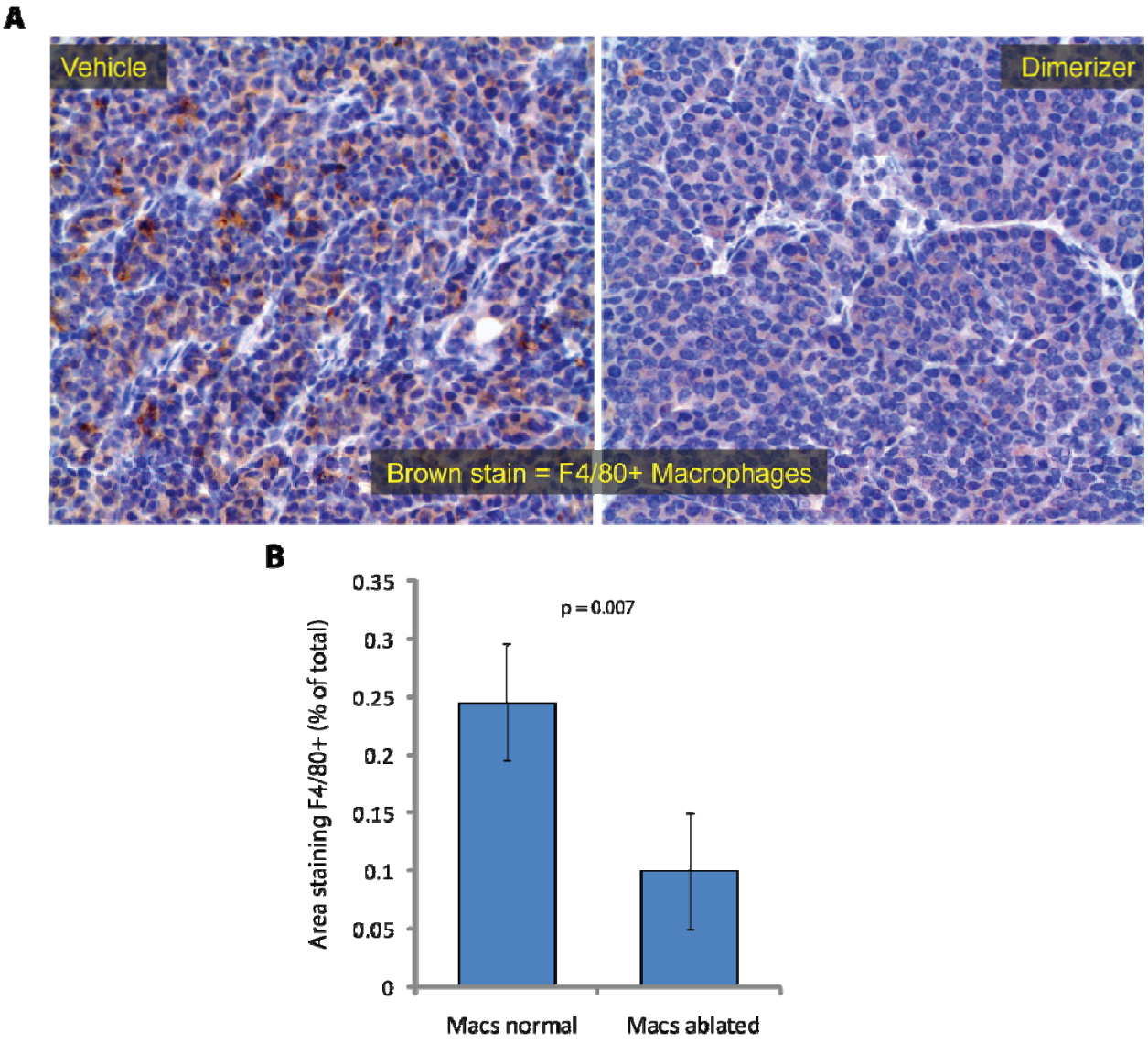

Administration of dimerizer eliminates macrophages from the tumors of MAFIA+, MMTV-PyMT+ mice. A) Tumors were removed from MAFIA+, PyMT+ mice treated with vehicle or dimerizer. Sections stained with antibodies directed at the F4/80 antigen reveal a relative paucity of macrophages throughout most of the tumors in mice treated with dimerizer. B) Sections of tumors from the same mice were stained by immunofluorescence and whole sections imaged using a fluorescent microscope fitted with a mechanized stage. Fluorescent pixel density was calculated using Adobe Photoshop CS3 software. For this analysis, n=3 mice per group, p=0.007 by Student's T test.

Figure 3

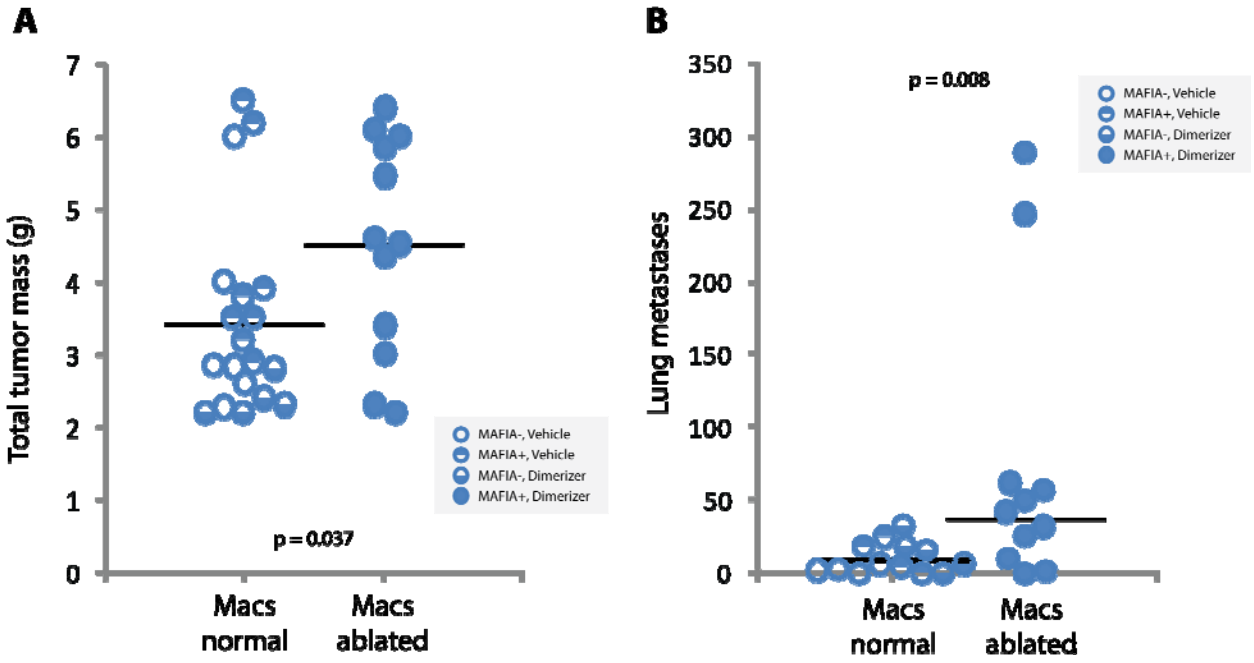

Macrophage ablation increases tumor size and accelerates metastasis. A) MAFIA+ or – mice were treated with vehicle or dimerizer according to the protocol outlined in methods. At euthanasia, all tumors were resected from the mice and weighed to calculate total tumor burden. MAFIA+ mice treated with dimerizer averaged tumors that were slightly larger than those from macrophage normal animals. For simplicity of analysis, and to avoid using unnecessary numbers of animals, mice are grouped into normal and macrophage ablated groups, though genotypes and conditions are shown on the graphs. p=0.037 by Student's T test, black lines show mean. B) Lungs extracted from these same animals were processed and analyzed as outlined in methods. MAFIA+ mice treated with dimerizer averaged more metastases than those with normal macrophages (p=0.008 by Mann-Whitney U, chosen for extreme values and non-standard distribution of counts). Black lines show median values.

Figure 4

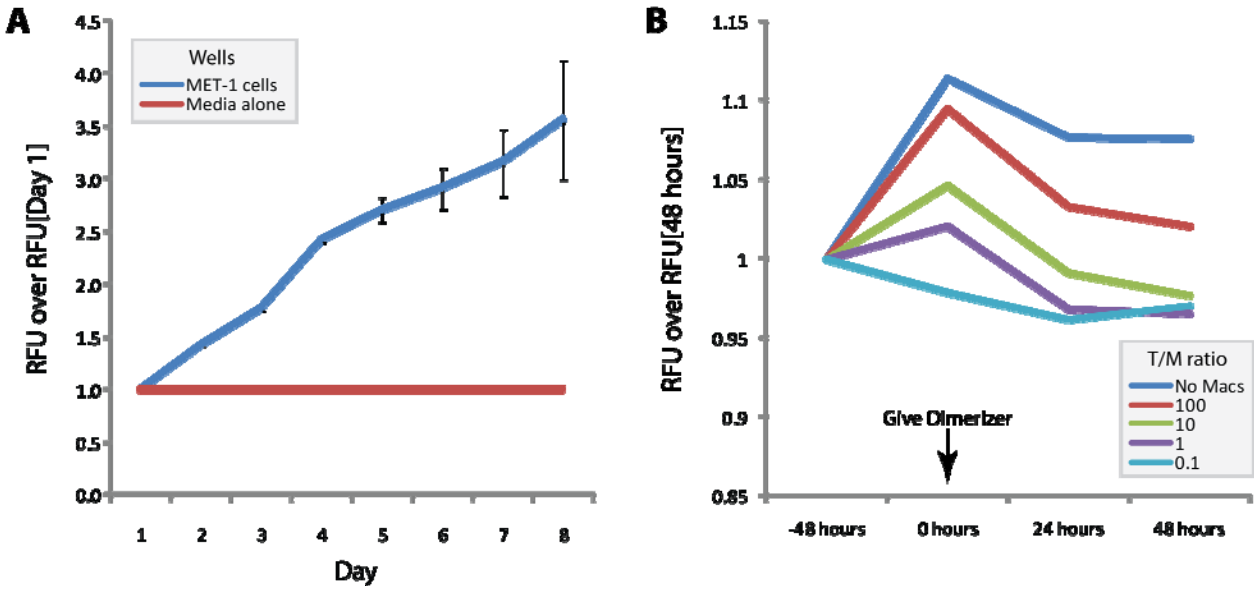

Tumor growth assays. A) This graph shows data validating the use of the newly-developed Met-1^{DsRed} cell line in the three-dimensional tumor growth assay (TGA). As the fluorescently-labeled cells multiply, the fluorescence intensity obtained by the plate reader increases proportionally. B) 12,500 Met-1DsRed cells per well were cultured alone (No Macs) or together with 125 (100), 1,250 (10), 12,500 (1), or 125,000 (0.1) MAFIA+ bone marrow-derived macrophages. After 48, all wells received dimerizer. These studies show that dimerizer, the apoptotic process, and/or the apoptotic bodies do not have any mitogenic effects on this PyMT tumor cell line. Studies were repeated three times per data point with bone marrow macrophages derived from three different donors. Error bars were omitted from this graph in the interest of clarity.

Figure 5

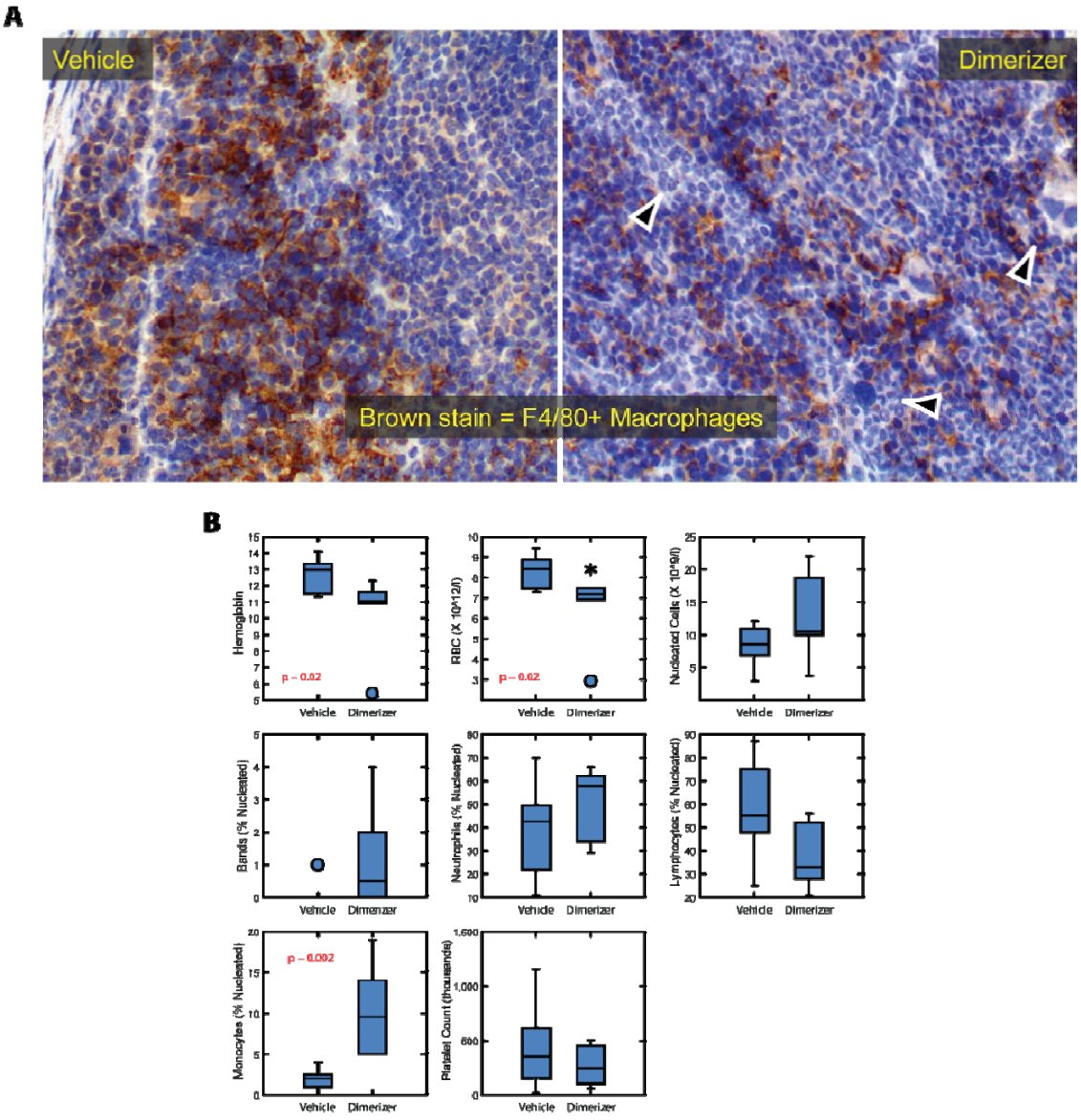

Macrophage ablation stimulates extramedullary hematopoiesis and a reactive monocytosis. A) Spleens taken from MAFIA+ mice treated with or without dimerizer were stained with antibodies directed at the F4/80 antigen. Macrophage-depleted mice show loss of splenic architecture and signs of extramedullary hematopoiesis (arrows). This evidence suggests a demand for the production of hematopoietic cells that cannot be met by the bone marrow. B) Graphs showing results of CBC analysis on the blood of tumor-bearing MAFIA+ mice treated for 5 weeks with vehicle or dimerizer. Macrophage-depleted mice display some evidence of anemia with a large reactive increase in blood monocyte levels. Statistical data shown represent Student's T test performed on 8 and 6 mice per group, respectively.

Figure 6

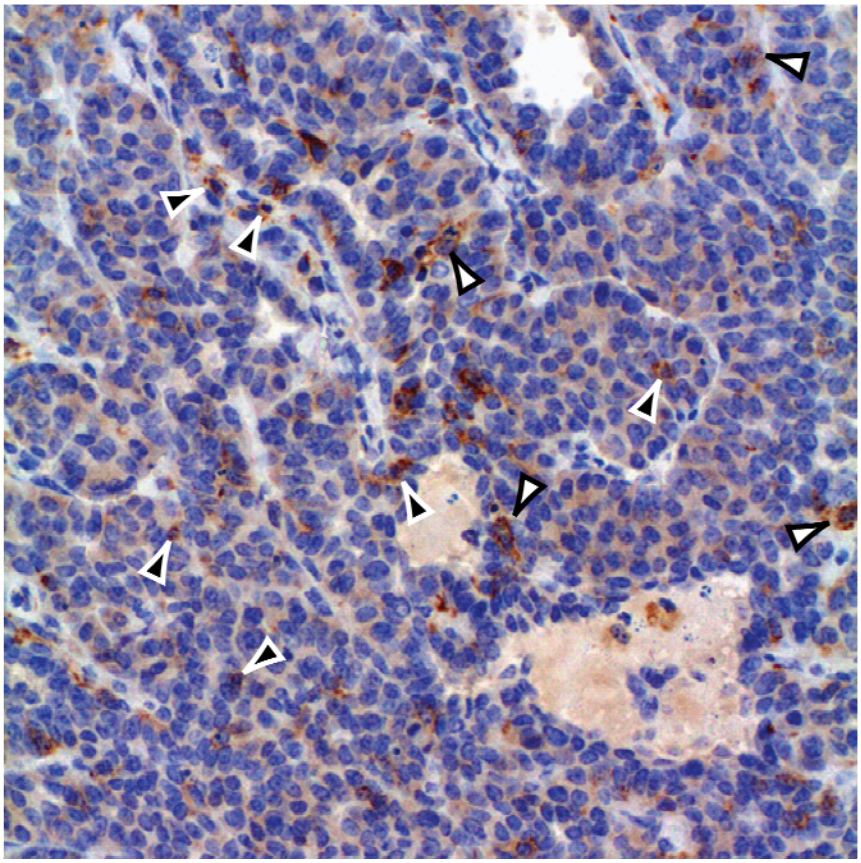

Tumors from macrophage-depleted mice show evidence of monocyte infiltration. Certain regions of the tumors from macrophage-depleted mice show patches of cells that stain positive for F4/80. Many of these patches, such as the one shown here, show a relatively large number of smaller, monocyte-like cells (black-center arrows). Many of the cells with more mature morphologies show signs of blebbing and apoptosis (white-center arrows).

Figure 7

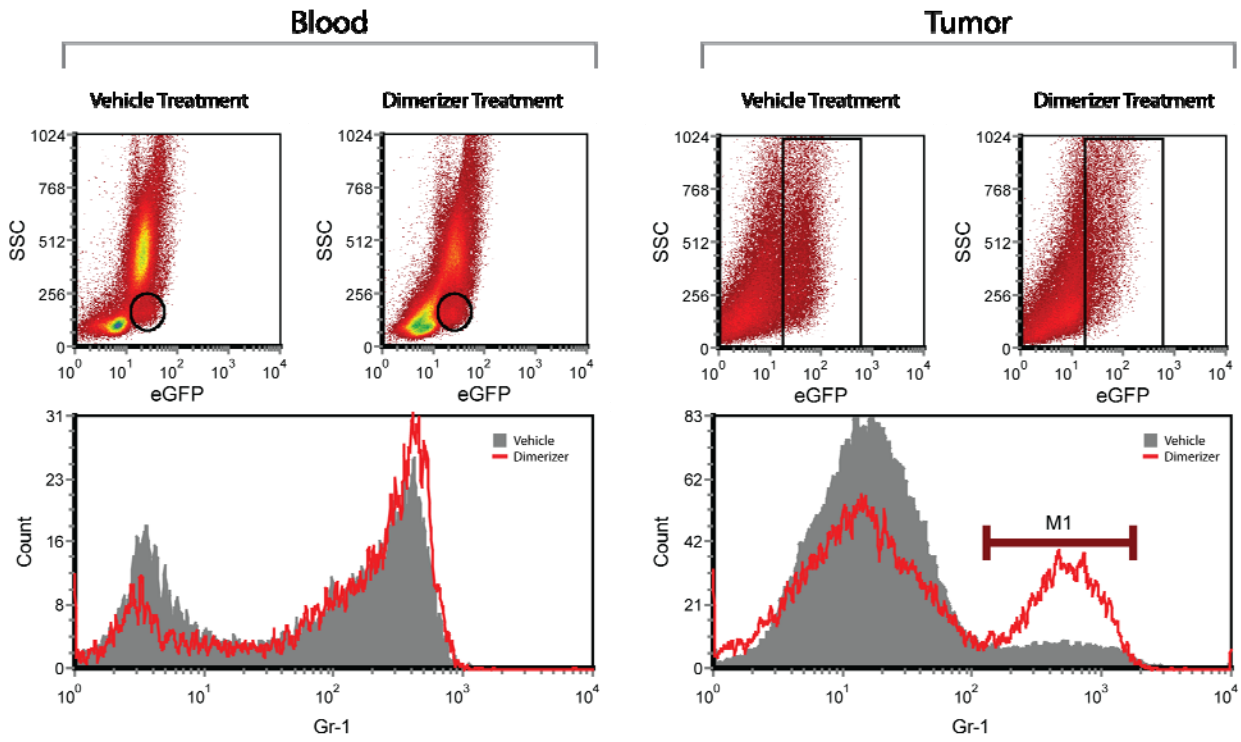

Mononuclear cells isolated from whole blood or tumors show a shift toward the Gr-1^{hi} phenotypes. Here, monocytes isolated from tumor-bearing mice show a shift from the normal 50-50 relative distribution of Gr-1^{hi} and Gr-1^{lo} populations (as evidenced by the gray graph showing monocytes isolated from mice treated with vehicle) to one enriched for the inflammatory, Gr-1^{hi} cells (averaging a 26 to 74 ratio in depleted mice). This trend continues in the mononuclear cells isolated from tumors, as evidenced in the graph on the right. Within the tumors, population distributions change from one that is 3.7% Gr-1^{hi} in mice treated with vehicle to one that is 29.6% Gr-1^{hi} in mice treated with dimerizer.